

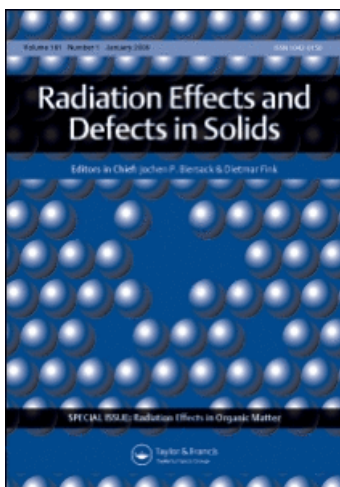
This article was downloaded by: [INFLIBNET India Order]

On: 6 October 2009

Access details: Access Details: [subscription number 909277354]

Publisher Taylor & Francis

Informa Ltd Registered in England and Wales Registered Number: 1072954 Registered office: Mortimer House, 37-41 Mortimer Street, London W1T 3JH, UK



## Radiation Effects and Defects in Solids

Publication details, including instructions for authors and subscription information:

<http://www.informaworld.com/smpp/title-content=t713648881>

### Response of Cellulose detectors to different doses of 62MeV protons

S. P. Tripathy<sup>a</sup>; R. Mishra<sup>a</sup>; K. K. Dwivedi<sup>b</sup>; S. Ghosh<sup>b</sup>; D. Fink<sup>b</sup>; D. T. Khathing<sup>c</sup>

<sup>a</sup> ANPA Italian National Agency for Environmental Protection Via V. Brancati 48 Roma Italy 00144. <sup>b</sup> Hahn-Meitner Institute Glienicke Strasse 100 Berlin Germany D-14109. <sup>c</sup> North-Eastern Hill University Department of Physics Shillong India 793 022.

Online Publication Date: 01 August 2003

**To cite this Article** Tripathy, S. P., Mishra, R., Dwivedi, K. K., Ghosh, S., Fink, D. and Khathing, D. T. (2003) 'Response of Cellulose detectors to different doses of 62MeV protons', *Radiation Effects and Defects in Solids*, 158:8,583 — 591

**To link to this Article:** DOI: 10.1080/1042015031000099753

**URL:** <http://dx.doi.org/10.1080/1042015031000099753>

PLEASE SCROLL DOWN FOR ARTICLE

Full terms and conditions of use: <http://www.informaworld.com/terms-and-conditions-of-access.pdf>

This article may be used for research, teaching and private study purposes. Any substantial or systematic reproduction, re-distribution, re-selling, loan or sub-licensing, systematic supply or distribution in any form to anyone is expressly forbidden.

The publisher does not give any warranty express or implied or make any representation that the contents will be complete or accurate or up to date. The accuracy of any instructions, formulae and drug doses should be independently verified with primary sources. The publisher shall not be liable for any loss, actions, claims, proceedings, demand or costs or damages whatsoever or howsoever caused arising directly or indirectly in connection with or arising out of the use of this material.

## RESPONSE OF CELLULOSE DETECTORS TO DIFFERENT DOSES OF 62 MeV PROTONS

S. P. TRIPATHY<sup>a,d,\*</sup>, R. MISHRA<sup>a,d</sup>, K. K. DWIVEDI<sup>b,c,†</sup>, S. GHOSH<sup>b</sup>,  
D. FINK<sup>b,‡</sup> and D. T. KHATHING<sup>d</sup>

<sup>a</sup>Italian National Agency for Environmental Protection, ANPA, Via V. Brancati 48, 00144-Roma, Italy; <sup>b</sup>Hahn-Meitner Institute, Glienicke Strasse 100, D-14109 Berlin, Germany; <sup>c</sup>Arunachal University, Rono Hills, Itanagar 791 111, India; <sup>d</sup>Department of Physics, North-Eastern Hill University, Shillong 793 022, India

(Received 25 October 2002; In final form 1 February 2003)

Optical and thermal responses of two cellulose detectors, Cellulose triacetate (Triafol-TN) and Cellulose acetate butyrate (Triafol-BN), to four different doses of 62 MeV protons were studied using spectroscopic, thermal and track-etching techniques. The spectroscopic analysis revealed that though the optical band-gap in the polymers was affected by proton irradiation, the polymers showed high resistance against any major structural modification by radiation. The thermal stability of the polymers was found to be affected by proton irradiation. The activation energy of etching was found to be almost constant for both the polymers even after irradiation. It is hoped that the findings in this work would be of significant relevance to material science and applications of polymers.

Keywords: Triafol-TN; Triafol-BN; Proton irradiation; Thermal stability; Cross-linking

### 1 INTRODUCTION

Radiation effects on polymer properties present valuable information for the investigation of the molecular structure and transport processes. Chain scission and cross-links as well as the mass-losses induced by electronic excitation and ionization are accepted as fundamental events that give rise to the observed macroscopic changes. A lot of work is in progress in the field of electron, gamma, proton and ion irradiation-induced modification in polymers [1–4]. An extensive study on the effect of proton irradiation on different polymers has been carried out. A decrease in thermal stability and an increase in track registration sensitivity of Polyallyldiglycol carbonate (PADC) was observed with an increase in the dose of 62 MeV protons [5]. A decrease in the optical band-gap and a simultaneous increase in the thermal stability was observed in 62 MeV proton-irradiated Polypropylene [6]. In the case of 62 MeV proton irradiation on Polytetrafluoro ethylene (PTFE), a stable free radical was traced from electron spin resonance spectroscopy which contributed to an increase in the optical conductivity of the polymer [7].

\* Corresponding author. E-mail: samtripathy@anpa.it

† E-mail: kkdau@rediffmail.com

‡ E-mail: fink@hmi.de

A decrease in activation energy for etching and an increase in crystallinity (X-ray diffraction analysis) was observed in Polyethylene terephthalate (PET) with an increase in the dose of 62 MeV protons [8]. In an extension of our investigation for improving the properties of polymers by proton irradiation, in the present work the response of two types of cellulose detectors, Cellulose triacetate (Triafol-TN) and Cellulose acetate Butyrate (Triafol-BN), has been studied.

Triafol-TN finds applications in manufacturing fibres, non-flammable safety cinematographic films, moulded articles, etc. Sinha et al. (1998) have found that gamma irradiation up to  $10^5$  Gy on TTN produces no change in the properties of TTN, but at  $10^6$  Gy the thermal stability decreased, the etch rate increased and TTN became brittle and turned to powder form [9]. UV radiation on TTN leads to the formation of conjugated double bonds which in turn gives rise to electron excitation levels in the visible spectral range and produces discolouration and reduction in light transmission [10].

Triafol-BN is a hard thermoplastic polymer having high impact strength, good dimensional stability and excellent compatibility with plasticisers. It has a much lower moisture absorption capacity as compared to Triafol-TN. It finds its applications in automobile components, safety goggles, etc. Sinha et al. (1998) have found that gamma irradiation up to a dose of  $10^5$  Gy on TBN produces no change in the polymer properties, but at  $10^6$  Gy TBN becomes brittle, the colour of the polymer fades due to destruction of purple dye, thermal stability decreases and the etch-rate increases [9].

In this work, the induced modifications in Triafol-TN and Triafol-BN are studied by spectroscopic, thermal and track-registration techniques.

## 2 EXPERIMENTAL DETAILS

### 2.1 Target Preparation and Proton Irradiation

Forty pieces of each Triafol-TN (composition  $C_{12}H_{16}O_8$ ; density  $1.15 \text{ g cm}^{-3}$ ; thickness  $100 \pm 0.1 \mu\text{m}$ ; colour blue) and Triafol-BN (composition  $C_{20}H_{32}O_5$ ; density  $1.20 \text{ g cm}^{-3}$ ; thickness  $200 \pm 0.1 \mu\text{m}$ ; colour violet) of sizes  $(1 \times 1) \text{ cm}^2$  were taken and eight stacks were prepared containing 10 pieces each. Each stack was covered by radiation-sensitive Polyvinylacetate (PVA) at both ends to check the uniformity of the impinging beam by its colour change. These were separately irradiated in the presence of air to four different doses, 10 kGy, 30 kGy, 60 kGy and 80 kGy, of 62 MeV proton in the Ion Beam Laboratory "ISL" of the Hahn Meitner Institute (HMI), Berlin. The collimated proton beam of dimension  $(0.3 \times 1) \text{ cm}^2$  passed perpendicularly through each stack. Then the pristine and the irradiated samples were characterised by the following techniques.

### 2.2 UV-Visible Spectroscopy

UV-Vis spectra for the pristine as well as irradiated Triafol-TN and Triafol-BN samples were obtained from a Beckman DU-650 spectrophotometer, in the wave-length region of 200–800 nm, at a scanning rate of 1200 nm/min. All the spectra were taken with pristine material as reference. The shift in absorption edges from UV to the visible region was correlated with the energy band-gap by Tauc's expression to calculate the energy band-gap [11].

### 2.3 Fourier Transform Infrared Spectroscopy (FT-IR)

The FT-IR spectra of all the samples were recorded in the wave number range of 4000 to  $500 \text{ cm}^{-1}$  using a Fourier transforming instrument (NICOLET, IMPACT 410) to study the

structural changes including the alteration in position and intensity of the characteristic bands with an accuracy better than  $\pm 1\%$  to  $\pm 3\%$ .

#### 2.4 Thermogravimetric Analysis (TGA)

The TGA thermograms were recorded by using the Perkin Elmer Delta series Thermal Analysis system. The samples were crimped in small aluminium pans and were heated from  $30^\circ\text{C}$  to  $800^\circ\text{C}$ . Analysis of the films was carried out under nitrogen purging using a scanning rate of  $20^\circ\text{C}/\text{min}$ . The error associated with TGA analysis is  $\pm 2^\circ\text{C}$ .

#### 2.5 Differential Scanning Calorimetry (DSC)

DSC measurements were performed by using the Perkin Elmer Delta series Thermal Analysis system. About 1–4 mg of samples were scanned in the calorimetry furnace in the temperature range  $50$ – $450^\circ\text{C}$ , with a heating rate of  $20^\circ\text{C}/\text{min}$ . A plot of heat flow as a function of temperature for DSC was obtained within the instrumental error of  $\pm 2^\circ\text{C}$ .

#### 2.6 Track Study

Both irradiated and pristine samples were further exposed to fission fragments from a  $^{252}\text{Cf}$  source at an angle of  $90^\circ$  for 30 minutes. Chemical etching of Triafol-TN and Triafol-BN samples was done in 3N and 6N NaOH solutions, respectively, at different etching temperatures of  $60^\circ\text{C}$ ,  $65^\circ\text{C}$ ,  $70^\circ\text{C}$  and  $75^\circ\text{C}$ . The samples were etched in 6 N NaOH solution, at different etching temperatures of  $60^\circ\text{C}$ ,  $65^\circ\text{C}$ ,  $70^\circ\text{C}$  and  $75^\circ\text{C}$ . The fission fragment diameters were measured with a Leitz optical microscope at  $625\times$  magnification at different etching times. The bulk etch-rate ( $V_G$ ) was then derived from the slope of the curve of increase of the fission track diameters versus etching time. The activation energy of the bulk etching rate was determined by plotting  $\log V_G$  against the reciprocal of the etching temperature. Mathematically,

$$\log V_G = \frac{-E_a}{2.303kT} + \log A \quad (\text{i})$$

where A is a constant,  $E_a$  is the activation energy for bulk etching in  $[\text{kJ mol}^{-1}]$ , k is the Boltzman's constant, and T is the absolute temperature in [K].

If m is the numerical value of the slope of the plot of  $\log V_G$  versus the reciprocal of etching temperature, then  $E_a$  can be given as:

$$E_a = 19.165 m. \quad (\text{ii})$$

### 3 RESULTS AND DISCUSSION

#### 3.1 UV-Visible Spectroscopy

The optical absorbance UV-Vis spectra of the two polymers revealed different characteristics. The absorption edge of the irradiated Triafol-TN shifted from UV towards the visible side, whereas in Triafol-BN, a shift of the absorption edge was observed from the higher towards the lower wavelength side. UV-Vis spectra of the pristine Triafol-TN and Triafol-BN along with the ones irradiated at the highest dose (80 kGy) are shown in Figure 1. The optical band-gap for the pristine as well as the irradiated polymers was calculated from

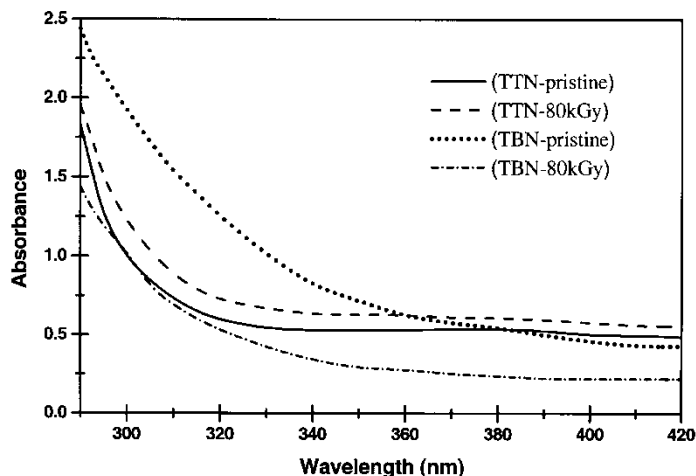


FIGURE 1 UV absorbance spectra of pristine Triafol-TN and Triafol-BN along with the samples irradiated at 80 kGy of 62 MeV protons.

the corresponding values of  $\lambda_g$  using the formula,  $E_g = hc/\lambda_g$ , where  $h$  is the Planck's constant and  $\lambda_g$  is the gap wavelength. The modification in the optical band-gap as a function of proton dose for both the polymers is shown in Figure 2. The optical band-gap ( $E_g$ ) for the pristine Triafol-TN was found to be 3.8 eV which slowly reduced with an increase in the dose of proton irradiation and reached a minimum of 3.4 eV at the highest dose (80 kGy). On the contrary, in Triafol-BN, a 33% increase in the optical band-gap was observed in the highest dose irradiated one, i.e.  $E_g$  for the pristine Triafol-BN was found to be 2.1 eV, which was found to increase with the dose to 2.8 eV at the highest dose.

### 3.2 Fourier Transform Infra-red Spectroscopy (FT-IR)

The identification of some of the characteristic absorbance peaks is made in Table I. Neither any significant change in the peak positions nor development of any new spectral

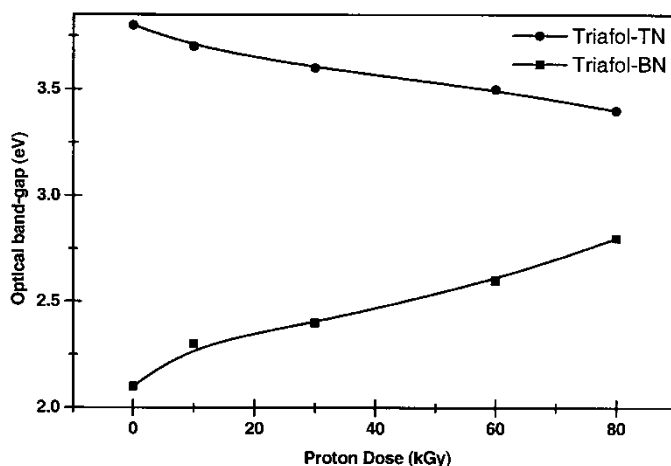


FIGURE 2 Modification in optical band-gap with increase in proton dose in both Triafol-TN and Triafol-BN.

TABLE I Identification of the Absorption Bands in TTN Corresponding to their Wavenumbers ( $1/\lambda$ ).

Peak	$1/\lambda$ , $\text{cm}^{-1}$	Identification
A	3530	COOH (or OH)
B	2951	C—H stretching
C	1723	C=O stretching from ester
D	1386	CH <sub>2</sub> —O scissors
E	1276	C—O—C stretching from ester
F	1187	Stretching vibration of the main chain
G	1080	C—O—C stretching from ester

characteristics was observed in the FT-IR spectra of the irradiated Triafol-TN and Triafol-BN. Most of the peak positions were found to be unshifted, only the absorbance or transmittance value of particular functional groups changed slightly. It implies that the inter-chain separation is not affected by proton irradiation in both the polymers. FT-IR analysis further confirmed the stability of these polymers against radiation degradation.

### 3.3 Thermogravimetric Analysis

The thermogravimetric analysis of the samples revealed the modification in thermal properties of the polymer that gives an insight into the structural modifications induced by ion irradiation. The TGA thermogram of Triafol-TN showed a 3-step decomposition process, i.e. slow decomposition zone with about 5% of weight-loss, fast decomposition zone with maximum weight-loss and a residual decomposition zone accompanied by 1–2% of weight-loss. As can be seen from the Figure 3, the stable zone (no weight-loss) was neither observed in the pristine polymer nor in the ones irradiated to lower doses (up to 30 kGy). It was presumably due to the decomposition of the blue dye from the polymer as soon as it was heated. The blue dye had already decomposed for the samples irradiated by higher doses (60 kGy and 80 kGy) and hence the stable zone was observed in those two samples till 170 °C. The temperatures corresponding to different decomposition zones are given in Table II. It was

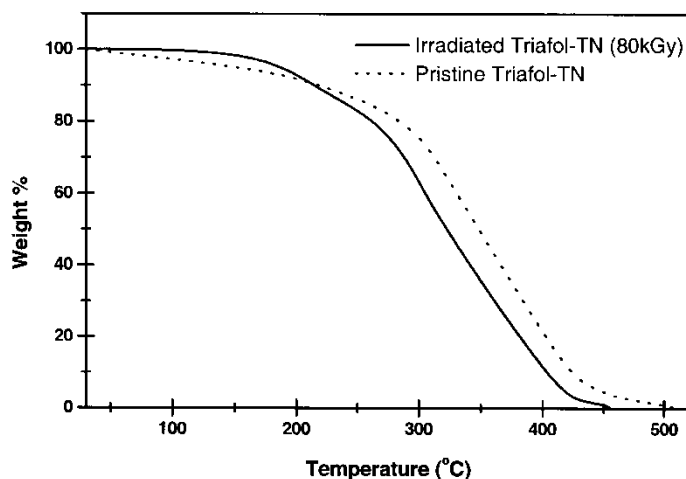


FIGURE 3 TGA thermogram of the pristine and the irradiated (80 kGy) Triafol-TN.

TABLE II Thermal Decomposition Temperatures at Different Zones (S-Stable Zone, SD-Slow Decomposition Zone, FD-Fast Decomposition Zone) for TTN and TBN Samples Irradiated to Different Doses (10, 30, 60, 80 kGy).

Dose (kGy)	Triafol-TN			Triafol-BN		
	S-zone, °C	SD-zone, °C	FD-zone, °C	S-zone, °C	SD-zone, °C	FD-zone, °C
0	–	30–300	300–410	–	30–322	322–425
10	–	30–297	297–409	30–180	180–322	322–415
30	–	30–297	297–405	30–180	180–322	322–415
60	30–170	170–295	295–400	30–180	180–322	322–410
80	30–170	170–290	290–400	30–180	180–290	290–406

observed that the fast decomposition zone in the pristine polymer started at around 300 °C and terminated at 410 °C, followed by a residual decomposition till 520 °C. The temperature of the fast decomposition zone decreased with an increase in the proton dose. In the sample irradiated by 80 kGy the fast decomposition zone was observed from 290–400 °C.

A similar behavior was also observed in the case of Triafol-BN. No stable zone was observed in the pristine sample probably due to decomposition of the violet dye when it was heated. But all the irradiated samples exhibited stable zones till 180 °C. The fast decomposition zone in the pristine Triafol-BN was observed in the temperature range of 322–425 °C followed by a residual decomposition. In the case of irradiated samples, it was observed that the decomposition zone decreased with an increase in the proton dose, the same as in the case of Triafol-TN. The temperatures corresponding to different decomposition zones for the pristine and the irradiated Triafol-BN are tabulated in Table II.

The decrease in the temperature corresponding to the fast decomposition zone with an increase in the proton dose in both the polymers indicated that though both the polymers are resistant to ionising radiation, the proton irradiation had resulted in some chain-scission in both polymers.

#### 3.4 Differential Scanning Calorimetry (DSC)

DSC thermograms (Fig. 4) indicate the modification in temperature of thermal transitions of the polymer before and after irradiation. The DSC curve is characterised by three major transitions—glass transition temperature, crystallisation temperature and melting temperature. Above the glass transition temperature the polymer has a high heat capacity. The polymer segments gain enough energy to move in ordered arrangements so that they start emitting heat resulting in an exothermic transition (crystallisation temperature,  $T_c$ ). When the sample is further heated above  $T_c$ , at a certain temperature (melting temperature,  $T_m$ ), the polymer chains absorb heat, come out of their ordered arrangements and the polymer undergoes an endothermic transition.

The thermogram of pristine Triafol-TN showed  $T_c$  at 279 °C followed by  $T_m$  at 316 °C. The crystallisation temperatures ( $T_c$ ) in the irradiated Triafol-TN samples were observed to decrease with the increase in proton dose at 260 °C for the sample irradiated at 60 kGy. For the sample irradiated at the highest dose of proton (80 kGy),  $T_c$  was not observed at all. The melting temperature in the pristine sample was recorded at 316 °C, which was also found to decrease with the increase in proton dose at 310 °C for the one irradiated at the highest dose (80 kGy).

In the case of pristine and irradiated Triafol-BN samples, the exothermic transition of crystallisation was not observed. It might be because the polymer segments do not gain enough heat to exhibit the crystallisation transition. Only an endothermic transition indicating the

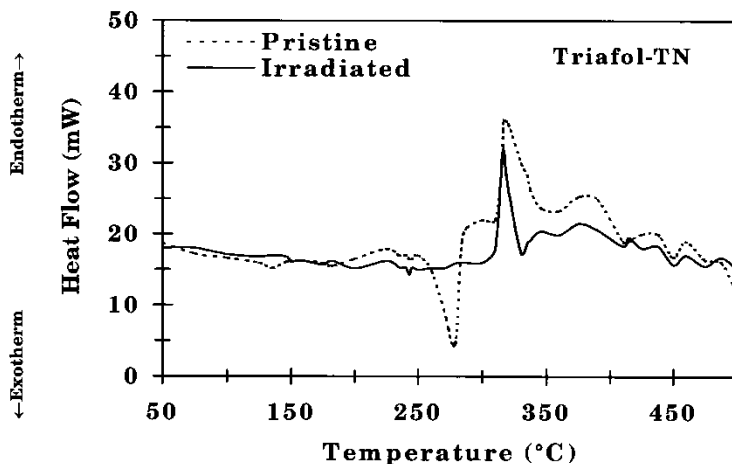


FIGURE 4 DSC thermogram of the pristine and the irradiated (80 kGy) Triafol-TN.

melting temperature was observed in the pristine sample at 334 °C, which reduced with the increase in proton dose and was observed at 321 °C for the one irradiated at the highest dose.

The temperatures corresponding to the thermal transitions as derived from the DSC thermograms are shown in Table III for both Triafol-TN and Triafol-BN. The decrease in area of the endothermic transition in the case of Triafol-TN as compared with the area of the pristine sample (as shown in Fig. 4) indicates that scissions induced by irradiation generate small chains which are more volatile and are consequently released at lower temperatures. So the DSC thermal analysis further supports the TGA analysis that the proton irradiation has resulted in some chain-scission in both the polymers.

### 3.5 Track Studies

The modification in the etching characteristics of both the polymers after the irradiation was investigated by this technique. The fission fragment track diameters were measured and plotted against the corresponding etching times to determine the bulk etch-rate ( $V_G$ ). The log of  $V_G$  was plotted against the reciprocal of different etching temperatures to calculate the activation energy ( $E_a$ ) of etching. The measured values of  $V_G$  for both Triafol-TN and Triafol-BN as a function of the etching temperature at different doses of proton are given

TABLE III The Temperature of Crystallisation ( $T_c$ ) (Exothermal Transition) and Melting ( $T_m$ ) (Endothermal Transition) in Pristine and Proton Irradiated Triafol-TN and Triafol-BN at Different Doses (10, 30, 60, 80 kGy).

Dose kGy	Triafol-TN		Triafol-BN $T_m$ , °C
	$T_c$ , °C	$T_m$ , °C	
0	279	316	334
10	265	313	328
30	265	313	326
60	260	312	323
80	-	310	321

TABLE IV The Bulk Etch-Rates ( $V_G$ ) of TTN and TBN as a Function of Different Doses of 62 MeV Protons (10, 30, 60, 80 kGy) and also as a Function of Different Etching Temperatures ( $T_{etch}$ ) and the Activation Energy of Etching ( $E_a$ ).

$T_{etch}$ , °C	$V_G$ ( $\mu\text{m}/\text{h}$ ) at different doses (kGy) of proton									
	TTN					TBN				
	0	10	30	60	80	0	10	30	60	80
60	1.7	1.8	1.8	1.8	1.9	0.6	0.7	0.7	0.8	1.0
65	2.3	2.3	2.3	2.4	2.5	0.9	1.0	1.0	1.2	1.5
70	3.1	3.2	3.2	3.2	3.3	1.5	1.7	1.7	1.9	2.2
75	4.0	4.2	4.2	4.2	4.3	2.3	2.5	2.6	2.9	3.6
$E_a$ , $\text{kJ mol}^{-1}$	53.4	53.4	53.4	53.4	53.0	81.1	81.3	81.3	81.2	81.2

in Table IV. The bulk etch-rate ( $V_G$ ) and the activation energy ( $E_a$ ) remained almost the same for the pristine and the irradiated Triafol-TN. So the proton irradiation was not able to significantly improve the track etching response of the polymer.

In the case of Triafol-BN, no significant increase in  $V_G$  was observed till the dose of 30 kGy, but was found to increase by about 30% for the sample irradiated to 60 kGy and by about 50% for the one irradiated at 80 kGy of 62 MeV proton. As can be seen from Table IV,  $E_a$  was found to be almost constant for Triafol-BN as well. So the proton irradiation accelerated the etching process without having any significant effect on the activation energy.

#### 4 CONCLUSION

Using techniques like UV-Vis spectroscopy, Fourier transform IR spectroscopy, thermogravimetric analysis, differential scanning calorimetry and track registration, the modifications on the different properties of Triafol-TN and Triafol-BN after 62 MeV proton irradiation are analysed as a function of the absorbed dose. UV-Vis spectral analysis revealed a decrease in the optical band-gap of Triafol-TN with an increase in the proton dose, whereas an increase in the same was observed for Triafol-BN. FT-IR spectroscopy confirmed the stability of the polymers against radiation degradation. Thermal analysis (TGA and DSC) showed that though the polymers are radiation-resistant, some chain-scission had occurred after irradiation. Proton irradiation failed to have any impact on the activation energy of etching in any of the polymers.

#### Acknowledgements

The authors thank the technical staff of ISL, HMI for proton irradiations. KKD thanks DAAD, Bonn for the fellowship under the re-invitation programme. SPT and RM thank the International Center for Theoretical Physics for the postdoctoral fellowship grants under the ICTP-TRIL programme. SG thanks DST for the fellowship grant under the BOYSCAST programme.

#### References

- [1] Senna, M. M., Abdel-Hamid, H. M. and Hussein, M. A. (2002). Nucl. Instr. and Meth. B, 187, 45.
- [2] Luck, H. B. (1982). Nucl. Instr. and Meth., 202, 497.

- [3] Evelyn, A. L., Ila, D., Zimmerman, R. L., Bhat, K., Poker, D. B., Hensley, D. K., Klatt, C., Kalbitzer, S., Just, N. and Derevet, C. (1999). Nucl. Instr. and Meth. B, 148, 1141.
- [4] Popok, V. N., Karpovick, I. A., Odzhaev, V. B. and Viridov, S. (1999). Nucl. Instr. and Meth. B, 148, 1106.
- [5] Tripathy, S. P., Mishra, R., Dwivedi, K. K., Khathing, D. T., Ghosh, S. and Fink, D. (2001). Radiation Measurements, 34, 15.
- [6] Tripathy, S. P., Mishra, R., Dwivedi, K. K., Khathing, D. T., Ghosh, S. and Fink, D. (2002). Radiation Measurements, 35, 95.
- [7] Tripathy, S. P., Mishra, R., Dwivedi, K. K., Khathing, D. T., Ghosh, S. and Fink, D. (2002). Radiation Effects and Defects in Solids, 157, 303.
- [8] Tripathy, S. P., Mishra, R., Dwivedi, K. K., Khathing, D. T., Ghosh, S. and Fink, D. (2002). Radiation Effects and Defects in Solids, 157, 387.
- [9] Sinha, D., Sarker, G. K., Ghosh, S., Kulshreshtha, A., Dwivedi, K. K. and Fink, D. (1998). Radiation Measurements, 29, 599.
- [10] Nouh, S. A. (1997). Radiation Measurements, 27, 499.
- [11] Mishra, R., Tripathy, S. P., Sinha, D., Khathing, D. T., Dwivedi, K. K., Ghosh, S., Muller, M., Fink, D. and Chung, W. H. (2000). Nucl. Instr. and Meth. B, 168, 59.